Long-Bone Fracture Detection in Digital X-ray Images Based on Concavity Index

Oishila Bandyopadhyay[1], Arindam Biswas[1], and Bhargab B. Bhattacharya[2]

[1] Department of Information Technology, Bengal Engineering and Science University, Howrah

[2] Center for Soft Computing Research, Indian Statistical Institute, Kolkata

Abstract. Fracture detection is a crucial part in orthopedic X-ray image analysis. Automated fracture detection for the patients of remote areas is helpful to the paramedics for early diagnosis and to start an immediate medical care. In this paper, we propose a new technique of automated fracture detection for long-bone X-ray images based on digital geometry. The method can trace the bone contour in an X-ray image and can identify the fracture locations by utilizing a novel concept of concavity index of the contour. It further uses a new concept of relaxed digital straight line (RDSS) for restoring the false contour discontinuities that may arise due to segmentation or contouring error. The proposed method eliminates the shortcomings of earlier fracture detection approaches that are based on texture analysis or use training sets. Experiments with several digital X-ray images reveal encouraging results.

Keywords: Medical imaging, Bone X-ray, Chain code, Digital straight line segment (DSS), Approximate digital straight line segment (ADSS).

1 Introduction

Fracture detection in X-ray images is an important task in emerging health-care automation systems [8], [6], [10]. Automated fracture identification from an orthopedic X-ray image needs extraction of the exact contour of the concerned bone structure. A fractured long-bone contour appears with irregular (uneven) or disconnected contour in the broken region. Bone contour discontinuity may also arise due to over-thresholding during segmentation of bone region from the surrounding flesh tissues and muscles. Long-bone fracture is a very common health problem, which needs immediate medical attention. A considerable number of men and women suffer from osteoporotic or accidental long-bone fracture everyday. Automated fracture detection can help the doctors and radiologist by screening out the obvious cases and by referring the suspicious cases to the specialists for closer examinations. Since bone fractures can occur in many ways, a single algorithm may not be suitable for analyzing the various types of fractures accurately. In the past, several approaches had been proposed by the researchers for detection of fractures in different bone regions.

Long-bone fractures usually refer to injuries in bones like humerus, radius and ulna, femur, tibia, and fibula. Each long-bone is divided into three regions

R.P. Barneva, V.E. Brimkov, and J. Šlapal (Eds.): IWCIA 2014, LNCS 8466, pp. 212–223, 2014.

- proximal, distal (two extremities), and diaphyseal [13]. A fracture of the diaphyseal is classified into three groups - simple, wedge, and complex. Tian et al. [16] has implemented a femur fracture detection approach by computing the angle between the axis of the neck of femur and the axis of the shaft. But this kind of method can only work on severe fractures that have caused a significant change in the angle of the neck and shaft of the femur. Another femur fracture detection approach uses contour generation and contour region filling followed by Hough-transform, vertical integral projection, and statistical projection of differential curve to identify the fractured region [17]. Donnelley et al. [7] have proposed a CAD system for the long-bone fracture detection which uses scale-space approach for edge detection, parameter approximation using Hough transform, diathesis segmentation followed by fracture detection using gradient analysis. Classification, a frequently used data mining technique, has also been used widely to detect the presence of fracture for the past few decades. These systems combine various features (like shape, texture, and colour) extracted from X-ray images and deploy machine learning algorithms to identify fractures [11]. Several researchers have proposed texture analysis of bone structure or bone mineral density estimation along with higher order statistical analysis for fracture detection [5], [14], [12].

In this paper, we have proposed a new technique based on relaxed digital straight line segment (RDSS) to restore the contour discontinuity that may arise during segmentation. Next, we use the corrected contour for identifying the fracture locations using the concept of concavity index of a digital curve. The proposed algorithm uses an entropy-based segmentation method [2] with adaptive thresholding-based contour tracing [1] to generate the bone contour of an X-ray image. The novelty of the technique lies in the fact that it rectifies the false discontinuities of a bone contour and identifies the fracture region correctly. Experiments on several long-bone digital X-ray images demonstrate the suitability of the proposed method for fracture related abnormality analysis.

2 Related Definitions

A digital image consisting of one or more objects, whose contour is formed with fairly straight line edges, can be represented by a set of (exact or approximate) digital straight line segments (DSS or ADSS). Such representations capture a strong geometric property that can be used for shape abstraction of these objects [3]. In the proposed algorithm, some properties of DSS are utilized for contour correction of a bone image. A few definitions related to this work are given below:

Digital Curve (DC). A DC C is an ordered sequence of grid points (representable by chain codes) such that each point (excepting the first one) in C is a neighbor of its predecessor in the sequence [15] (see 2(b), 2(c)).

Chain Code. It is used to encode a direction around the border between pixels. If $p(i, j)$ is a grid point, then the grid point (i', j') is a neighbor of p, provided that $max(|i-i'|, |j-j'|) = 1$. The chain code [9] of p with respect to its neighbor grid point in C can have a value in $0, 1, 2, ..., 7$ as shown in Fig. 2 (a).

Digital Straight Line Segment (DSS). The main properties of DSS [15], [3] are:
(F1) The runs have at most two directions, differing by 45^0, and for one of them, the run length must be 1.
(F2) The runs can have only two lengths, which are consecutive integers.
(F3) One of the run lengths can occur only once at a time.

The necessary and sufficient conditions for a digital curve (DC) to be a DSS have been stated in the literature [15], [3]. In [15], it has been shown that a DC is the digitization of a straight line segment if and only if it has the chord property. A DC C has the chord property if, for every (p, q) in C, the chord pq (the line segment drawn in the real plane, joining p and q) lies near C, which, in turn, means that, for any point (x, y) of pq, there exists some point (i, j) of C such that $max(|i - x|, |j - y|) < 1$.

Relaxed Digital Straight Line Segment (RDSS). In this paper, we introduce the concept of Relaxed Digital Straight Line Segment, defined below:
RDSS inherits the basic property of the underlying DSS, i.e.,
(F1) At most two types of elements (chain code directions) can be present in a RDSS and these can differ only by unity, modulo eight.
Thus, a RDSS represents single pixel curve with very small curvature by a relaxed digital straight line. For example, in Fig. 1(b)), a portion of the curved line is approximated by two consecutive RDSS, R1 and R2.

A tighter condition leads to an earlier concept of Approximate Digital Straight Line Segment (ADSS) [3]. The main properties of ADSS are:
(F1) At most two types of elements can be present and these can differ only by unity, modulo eight.
(F2) One of the two element values always occurs singly.
(F3) Successive occurrences of the element occurring singly are as uniformly spaced as possible.

3 Proposed Algorithm

In an X-ray image, the bone parts appear along with the surrounding tissues or muscles (i.e., flesh). So bone region segmentation and bone contour generation is necessary for automated fracture identification process. The proposed method segments the bone region of input X-ray (Fig. 3(a)) image from its surrounding flesh using an entropy-standard deviation based segmentation method (Fig. 3(b)) and then applies an adaptive thresholding based technique to generate the bone contour [2][1] (Fig. 3(c)). Any discontinuity that appears in bone contour during segmentation, is corrected by the proposed method using RDSS (Fig. 3(d)). Bone fracture regions are then identified by analyzing concavity index of the corrected image (Fig. 3(e)).

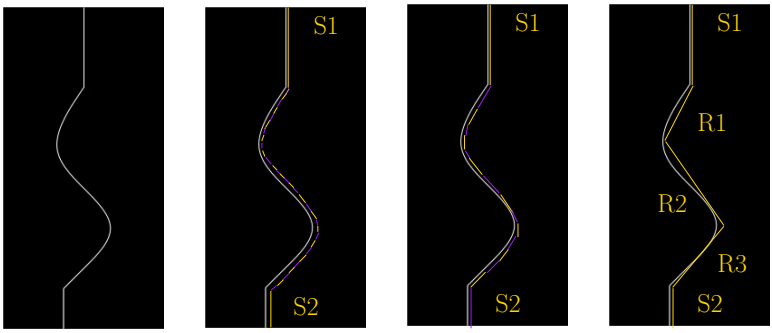

Fig. 1. RDSS (a) Straight line segment and curve, (b) corresponding DSS (35 segments), (c) corresponding ADSS (16 segments), (d) corresponding RDSS (5 segments)

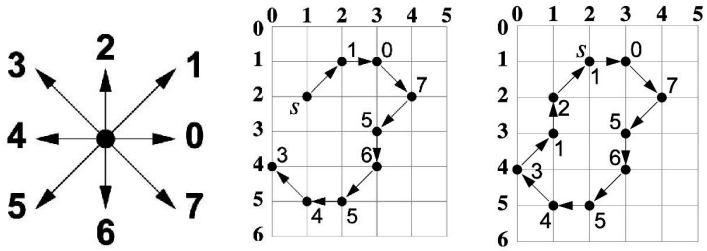

Fig. 2. Chain code (a) Chain code in 8-neighbor connectivity, (b) DC (1, 2)(10756543), (c) DC (2, 1)0756543121

3.1 Bone Region Segmentation from an *X*-ray Image

The major challenge in segmentation of bone region in any X-ray image lies in identification and extraction of flesh to bone transition region. Overlapping intensity range of flesh and bone region restricts the use of pixel-based thresholding or edge-based approaches as they often fail to produce accurate results. In the proposed algorithm, local entropy image is generated from the input X-ray image [2]. Local entropy image clearly identifies the flesh-bone transition points in a X-ray image with bright bone region and relatively darker flesh region. However, some X-ray images appear with bright flesh region resulting in overlapping flesh and bone intensity range. In such cases, the entropy image often fails to identify the flesh to bone transition correctly. To overcome this problem, we compute local standard deviation for each pixel and multiplied it with local entropy to facilitate bone image segmentation [1].

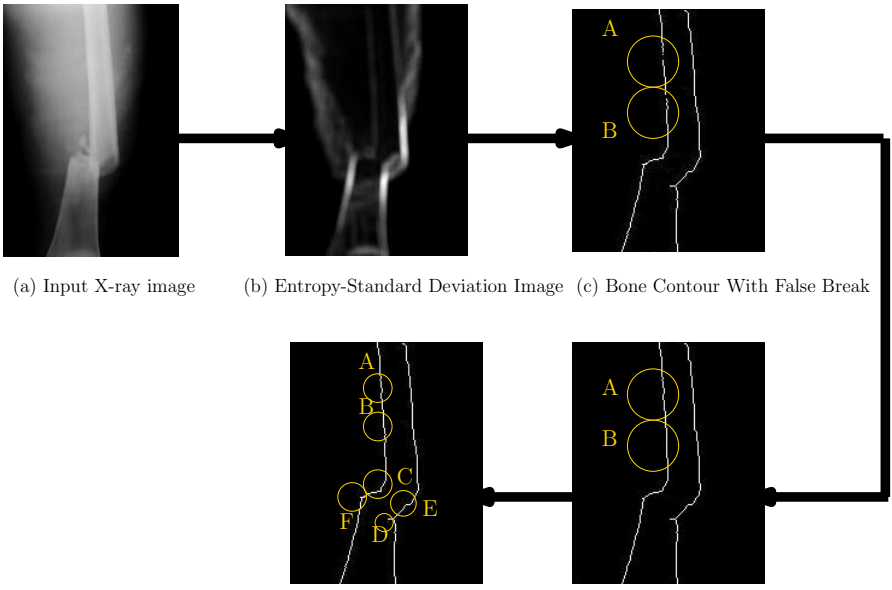

(a) Input X-ray image (b) Entropy-Standard Deviation Image (c) Bone Contour With False Break

(e) Detected Fracture Locations (d) Contour Corrected Image

Fig. 3. Different phases of proposed algorithm

3.2 Contour Generation Using Adaptive Thresholding

The proposed approach generates the bone contour from a segmented bone image (entropy-standard-deviation image) using an adaptive thresholding method [1]. In adaptive thresholding based bone contour generation technique, the segmented bone image J is traversed using a small window. For each pixel α of J, the window is constructed with its 8 neighboring pixels. The window is divided into four cells, top-left (C_1), top-right (C_2), bottom-left (C_3) and bottom-right (C_4). All these four cells are incident on α. To determine whether a cell C_i has a portion of bone boundary in it, adaptive thresholding approach is used [4]. The contour traversal algorithm checks the intensity values of neighboring pixels and selects the next pixel position whenever it encounters a pixel whose intensity value exceeds the adaptive threshold value of the present pixel. After selection of a new pixel position, the algorithm checks whether or not the pixel is already visited. If the pixel is found visited, then the algorithm starts searching from a new position; otherwise it adds the current pixel in the visited list and decides the direction for the next move [1].

3.3 Contour Correction Using Relaxed Digital Straight Line Segments

A bone fracture may cause a disconnected or irregular (uneven) bone contour. Hence, any discontinuity in the bone contour that appears during segmentation

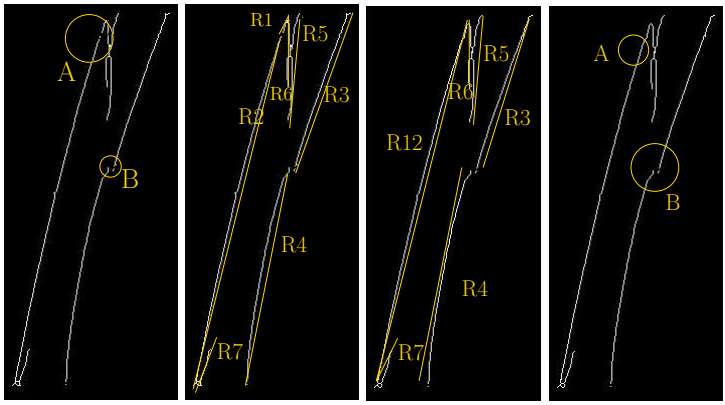

Fig. 4. Contour correction (a) Bone contour with false break, (b) Contour with RDSS, (c) Corrected contour with RDSS, and (d) Corrected contour

or contour generation, can mislead fracture detection . To overcome this problem, we propose a novel approach based on relaxed digital straight line segment (RDSS).

In the proposed method, the bone contour generated using adaptive thresholding approach is traversed from top-left to bottom and from bottom-right to top and the corresponding chain code list is generated. This chain code list is analyzed to approximate the underlying curve with relaxed digital straight line segments (RDSS). If any discontinuity arises in bone contour during segmentation or contour generation process (see region A of Fig. 4(b)), then it should have been be covered by two different RDSS. The proposed algorithm searches for all such RDSS pairs that cover the bone contour with same or its complementary chain code string. For example, a RDSS with chain code consisting of {1,2} can be paired with another having the code {5,6} as the RDSS covering the two line segments across the break will be traversed either from the same (or opposite) direction, with the start and end pixels lying in close neighborhood of each other. After finding such RDSS pairs, any one of these two RDSS is extended in the direction of traversal to connect them into a single RDSS (see Fig. 4(c). Any discontinuity in the bone contour caused by a fracture (see region B of Fig. 4(d)) will change their alignment. Therefore, a RDSS cover of such discontinuities cannot be extended to combine them into a single RDSS. On the other hand, the contour discontinuities caused by segmentation or contouring errors can be corrected by projecting the two neighboring RDSS towards each other.

Approximation of a bone contour can also be performed using DSS or ADSS; however, the number of segments required to cover the contour would be very high as in a single-pixel wide long-bone image, the contour usually changes the direction at an interval of every 5 to 10 pixels. Thus the use of RDSS not only reduces the number of approximating straight line segments, but also rectifies the false breaks in the contour, while reporting the correct fracture locations (see Fig. 4(d)).

3.4 Fracture Detection Using Concavity Index

In the proposed algorithm, we introduce the concept of concavity index, which is used to detect the fractures in long-bones.

Concavity Index (α). During the traversal, each point p_i is assigned a concavity index, α_i where α_0 and α_1 are initialized to 0 and 1 respectively. To obtain α_{i+1}, α_i is incremented (decremented) by the difference of the directions, d_i and d_{i+1}, if the contour moves in clockwise (counter-clockwise) direction from p_i to p_{i+1}, where d_i is the incident direction at p_i.

It should be noted that if the curve propagates in the same direction, the concavity index remains unchanged, however, a significant variation of α indicates abnormalities in the curve leading to fracture detection.

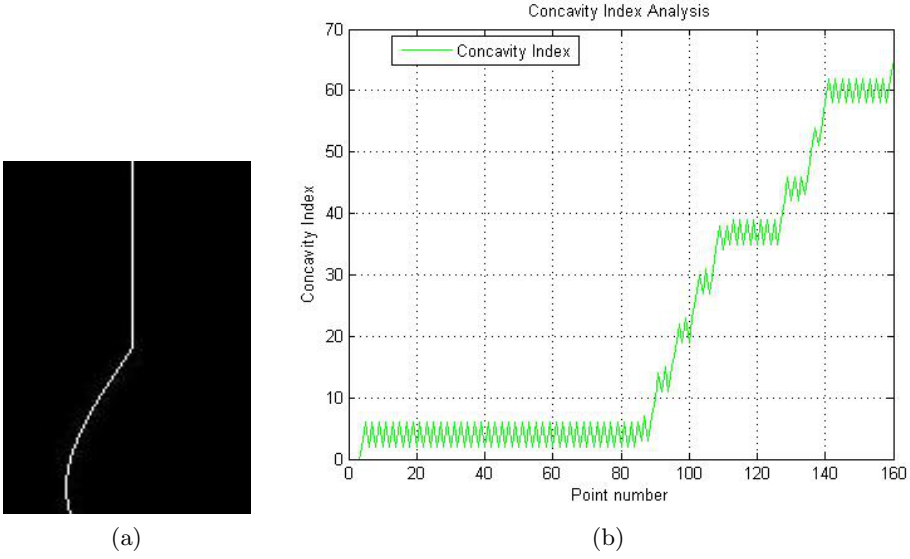

Fig. 5. Concavity Index (a) A line with straight and curved region, (b) Concavity indices of different points of the curve shown in (a)

In the above example (Fig. 5), it is clearly shown that concavity index changes significantly in a curved region. The proposed method uses this property of concavity index in fracture detection of long-bone contour.

We traverse the bone contour chain code and computes the concavity index for all pixel positions during traversal. We plot concavity index against the pixel positions as we traverse the contour. In a fractured long-bone, the bone boundary appears as a curve in the fractured part of the contour as the abnormality therein degrades its straightness. The proposed algorithm thus locates the fractured regions by observing the sharp and frequent changes (wave-like structure with peak and fall) in concavity index value (see Fig. 6(b)). Experimental evidences show that

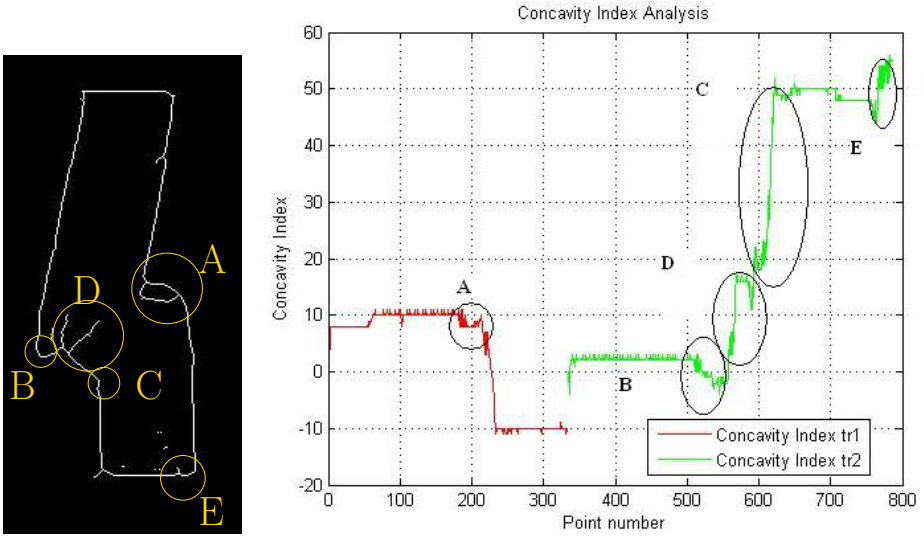

(a) (b)

Fig. 6. (a) Contour of input image with fracture marked (b) Concavity index plot for each traversal of (a) with marked changes in fracture location.

in the fractured regions, the change in chain code is more than 3 and change in concavity index exceeds 10 over a contour length of around 5 or 6 pixels. The groups of neighbouring pixels identified with such values are then clustered to identify the fracture zones marked in the concavity index curve (Fig. 6(b)). In this example, regions marked as 'A', 'B', 'C', 'D' identify the fractured region correctly and that marked as 'E' shows wrong identification (false positive).

4 Experimental Results

The proposed method is tested on several X-ray images of long-bone fracture. For each case, the concavity index curve is analyzed to identify the fractured locations. It is noticed that for most of the cases the fractured locations are identified correctly. Concavity index is computed during bone contour tracing from top-left corner to bottom and from bottom-right corner to top (plot with different colour in 7). A plot of concavity index against the traversed pixel list shows that the concavity index increases gradually (region 'A' in concavity index curve of Fig. 7(h)) during the traversal of regular bone curvature (as shown in region 'A' of Fig. 7(g)). A traversal of the fractured regions shows a fast change in te concavity index; this generates a wave like structure with peaks and falls in the curve (see region marked with 'A', 'B', 'C', 'D', 'E' of Fig 7(c)) and respective regions in concavity index curve (see region marked with 'A', 'B', 'C', 'D', 'E' of Fig 7(d)). Table -1 shows the concavity curve analysis for each X-ray image. It is noticed that the number of false positives identified in the fractured region

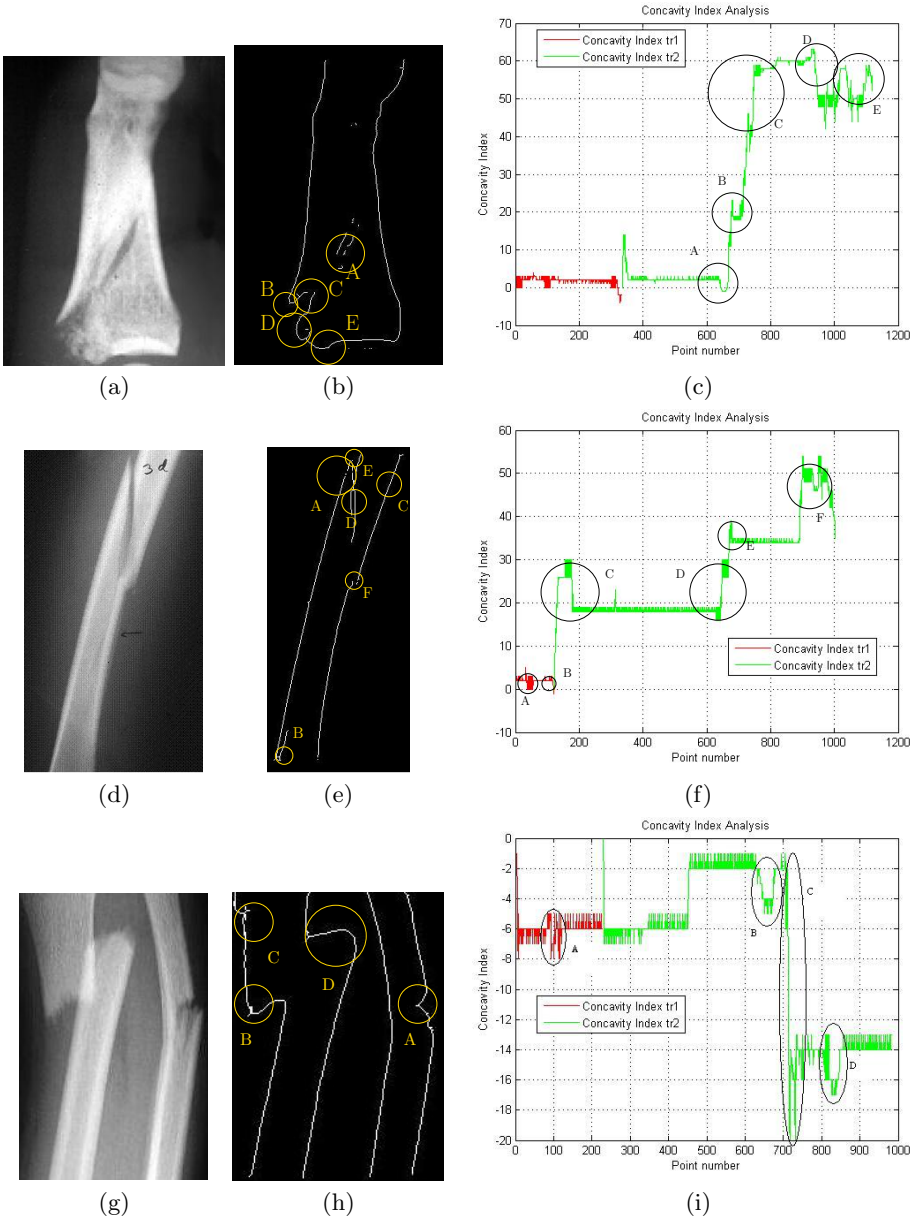

Fig. 7. (a) X-ray image (b) Contour of input image with fracture marked (c) Concavity index plot for each traversal of (a) with marked changes in fracture location; (d) X-ray image (e) Contour of input image with fracture marked (f) Concavity index plot for each traversal of (d) with marked changes in fracture location; (g) X-ray image (h) Contour of input image with fracture marked (i) Concavity index plot for each traversal of (g) with marked changes in fracture location

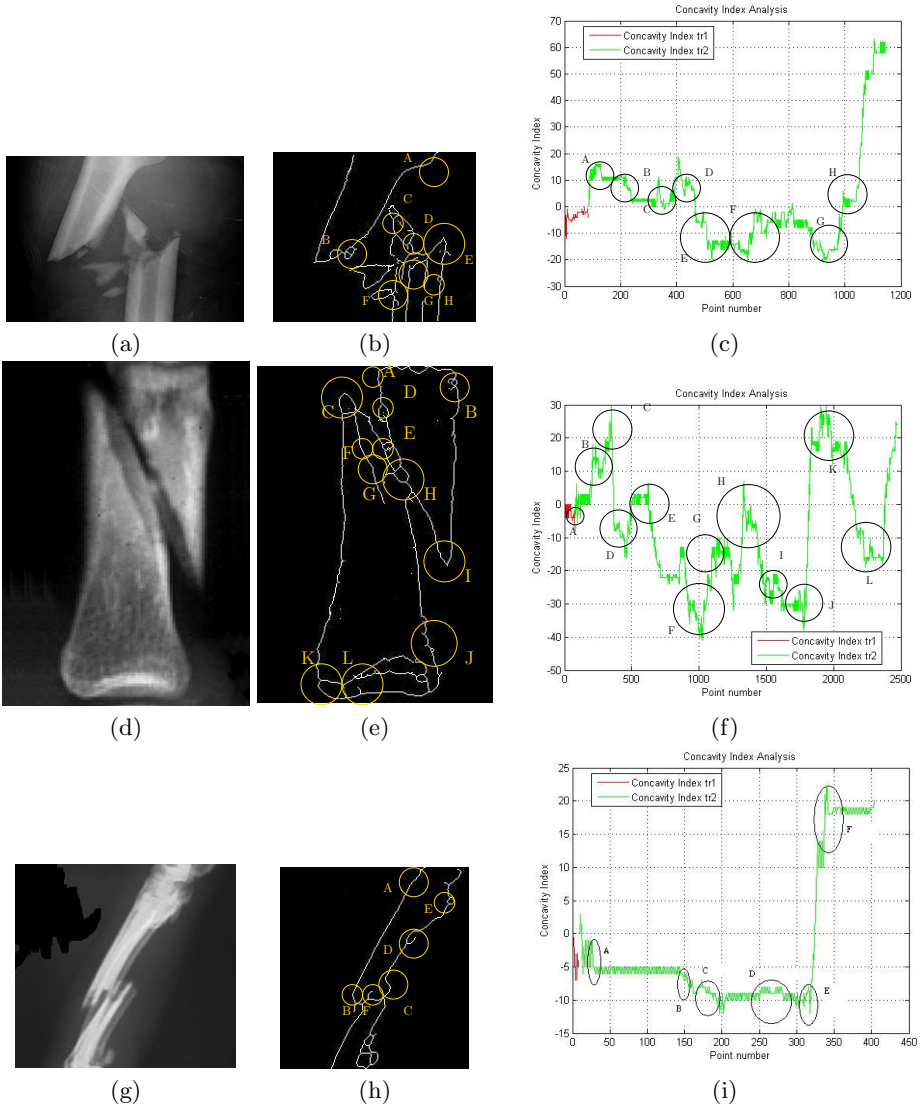

Fig. 8. Complex Fracture Identification (a) X-ray image (b) Contour of input image with fracture marked (c) Concavity index plot for each traversal of (a) with marked changes in fracture location; (d) X-ray image (e) Contour of input image with fracture marked (f) Concavity index plot for each traversal of (d) with marked changes in fracture location; (g) X-ray image (h) Contour of input image with fracture marked (i) Concavity index plot for each traversal of (g) with marked changes in fracture location

Table 1. Concavity Index Analysis for Fracture Detection in X-Ray Images

Input image	Fracture region identified	Correct identification	False positive
Fig. 6(a)	5	4 (A, B, C, D)	1 (E)
Fig. 7(b)	4	4 (B, C, D, E)	0
Fig. 7(e)	7	4 (A, D, E, F)	2 (C, B)
Fig. 7(h)	4	3 (A, B, D)	1 (C)
Fig. 8(b)	8	6 (B, C, D, E, F)	2 (A, H)
Fig. 8(e)	12	8 (A, C, D, E, F, G, H, I)	4 (B, J, K, L)
Fig. 8(h)	6	3 (B, C, F)	3 (A, D, E)

of each image is considerably low. Fig. 8 shows some example of more complex fractures where bones are fragmented into multiple pieces. The concavity curve of these X-ray images appears as multiple waves (see Fig. 8(c), Fig. 8(f), Fig. 8(i)), which clearly indicate the presence of fractures in the input image.

5 Conclusion

We have proposed a method for fracture detection in X-ray images based on digital geometry. We have shown, for the first time, that the power of digital geometric techniques can be harnessed to provide fast and accurate solutions to the automation of medical image analysis. Our experiments on several X-ray image databases demonstrate its suitability of fracture detection in long-bone structures.

References

1. Bandyopadhyay, O., Biswas, A., Chanda, B., Bhattacharya, B.B.: Bone contour tracing in digital X-ray images based on adaptive thresholding. In: Maji, P., Ghosh, A., Murty, M.N., Ghosh, K., Pal, S.K. (eds.) PReMI 2013. LNCS, vol. 8251, pp. 465–473. Springer, Heidelberg (2013)
2. Bandyopadhyay, O., Chanda, B., Bhattacharya, B.B.: Entropy-based automatic segmentation of bones in digital X-ray images. In: Kuznetsov, S.O., Mandal, D.P., Kundu, M.K., Pal, S.K. (eds.) PReMI 2011. LNCS, vol. 6744, pp. 122–129. Springer, Heidelberg (2011)
3. Bhowmick, P., Bhattacharya, B.B.: Fast polygonal approximation of digital curves using relaxed straightness properties. IEEE Transactions on Pattern Analysis and Machine Intelligence, 1590–1602 (2007)

4. Biswas, A., Khara, S., Bhowmik, P., Bhattacharya, B.B.: Extraction of region of interest from face images using cellular analysis. ACM Compute 2008, 1–8 (2008)
5. Chai, H.Y., Wee, L.K., Swee, T.T., Salleh, S.H., Ariff, A.K., Kamarulafizam: Gray-level co-occurrence matrix bone fracture detection. American Journal of Applied Sciences, 26–32 (2011)
6. Donnelley, M., Knowles, G.: Automated bone fracture detection. In: Proceedings of SPIE 5747, Medical Imaging: Image Processing, p. 955 (2005)
7. Donnelley, M., Knowles, G., Hearn, T.: A CAD system for long-bone segmentation and fracture detection. In: Elmoataz, A., Lezoray, O., Nouboud, F., Mammass, D. (eds.) ICISP 2008 2008. LNCS, vol. 5099, pp. 153–162. Springer, Heidelberg (2008)
8. Eksi, Z., Dandil, E., Cakiroglu, M.: Computer-aided bone fracture detection. In: Proceedings of Signal Processing and Communications Applications, pp. 1–4 (2012)
9. Freeman, H.: On the encoding of arbitrary geometric configurations. IRE Trans. Electronic Computers, 260–268 (1961)
10. Hacihaliloglu, I., Abugharbieh, R., Hodgson, A.J., Rohling, R.N., Guy, P.: Automatic bone localization and fracture detection from volumetric ultrasound images using 3-d local phase features. Ultrasound Med. Biol. (1), 128–144 (2012)
11. Lum, V.L.F., Leow, W.K., Chen, Y.: Combining classifiers for bone fracture detection in X-ray images. In: IEEE International Congress on Image and Signal Processing, 1149–1152 (2005)
12. Materka, A., Cichy, P., Tuliszkiewicz, J.: Texture analysis of X-ray images for detection of changes in bone mass and structure. In: Texture Analysis in Machine Vision. p. 257, World Scientific (2000)
13. Muller, M.E., Nazarian, S., Koch, P., Schatzker, J.: The comprehensive classification of fractures of long bones. Springer (1990)
14. Ouyang, X., Majumdar, S., Link, T.M., Lu, Y., Augat, P., Lin, J., Newitt, D., Genant, H.K.: Morphometric texture analysis of spinal trabecular bone structure assessed using orthogonal radiographic projections. Medical Physics Research and Practice, 2037–2945 (1998)
15. Rosenfeld, A.: Digital straight line segments. IEEE Transactions on Computers, 1264–1269 (1974)
16. Tian, T.-P., Chen, Y., Leow, W.-K., Hsu, W., Howe, T.S., Png, M.A.: Computing neck-shaft angle of femur for X-ray fracture detection. In: Petkov, N., Westenberg, M.A. (eds.) CAIP 2003. LNCS, vol. 2756, pp. 82–89. Springer, Heidelberg (2003)
17. Wei, Z., Liming, Z.: Study on recognition of the fracture injure site based on X-ray images. In: IEEE International Congress on Image and Signal Processing, pp. 1947–1950 (2010)